Journal of the Geological Society, *London*, Vol. **158**, 2001, pp. 769–784. Printed in Great Britain.

How to resist subduction: evidence for large-scale out-of-sequence thrusting during Eocene collision in western Turkey

KLAUS GESSNER[1,3], UWE RING[1], CEES W. PASSCHIER[1] & TALIP GÜNGÖR[2]

[1]*Institut für Geowissenschaften, Johannes Gutenberg-Universität, 55099 Mainz, Germany.*
[2]*Jeoloji Mühendisligi Bölümü, Dokuz Eylül Üniversitesi, 35100 Bornova, Turkey.*
[3]*Present address: CSIRO Exploration and Mining, PO Box 1130, Bentley WA 6102, Australia.*
(e-mail: klaus@ned.dem.csiro.au)

Abstract: Significant along-strike variations have locked large parts of the Alpine subduction complex in the Eastern Mediterranean in the Eocene, and defined the end of high-pressure accretion in western Turkey. Structural analysis reveals that the Anatolide belt in western Turkey formed under greenschist facies metamorphic conditions in the Eocene when a high-pressure metamorphic fragment of the Adriatic plate (the Cycladic blueschist unit) was thrust onto the imbricated mid-crustal units of the Anatolian microcontinent (the Menderes nappes). The contact between the Cycladic blueschist unit and the Menderes nappes, the Cyclades–Menderes thrust, represents an out-of-sequence ramp which cuts up-section towards the south. The lack of Alpine high-pressure fabrics below the Cyclades–Menderes thrust implies *c.* 35 km of exhumation of the Cycladic blueschist prior to its Eocene emplacement on top of the Menderes nappes. Structure and geodynamic evolution of the Anatolide belt are in striking contrast to the neighbouring Aegean and contradict the model of a laterally continuous orogenic zone, in which the Anatolide microcontinent is interpreted as an eastern extension of the Adriatic plate.

Keywords: Alpine orogeny, Turkey, Aegean Sea, metamorphism, thrust faults, exhumation.

The Hellenide–Anatolide orogen in the Eastern Mediterranean formed by Cretaceous to recent accretion of continental fragments to the active southern margin of Eurasia (Sengör & Yilmaz 1981; Robertson & Dixon 1984). Tectonic units within the Hellenide–Anatolide orogen are aligned parallel to the present-day Hellenic subduction zone, and have traditionally been regarded as an arcuate arrangement of laterally continuous orogenic belts (e.g. Brunn 1956; Aubouin 1959; Dürr *et al.* 1978; Jacobshagen *et al.* 1978). A fundamental assumption of this hypothesis is that the Pelagonian zone (Aubouin 1959), the Cycladic zone and the Menderes Massif (Paréjas 1940) can be grouped together as a continuous 'Median Crystalline Belt' (Dürr *et al.* 1978). In this 'classical' interpretation the Median Crystalline Belt represents Carboniferous basement and Permo-Mesozoic cover of the Adriatic plate (Fig. 1). It has recently been proposed that only the upper levels of the Menderes Massif (the 'Cycladic blueschist unit') were correlative with the Cycladic zone, while the lower units were formed by the exotic Menderes nappes (Ring *et al.* 1999*a*). The subdivision of these authors will be adapted in this paper, and the term 'Menderes Massif' will not be used in a tectonic context.

A striking characteristic of the Hellenides in the Aegean is the southward propagation of nappe emplacement and high-pressure metamorphism. In this paper, it will be shown how this propagation relates to the formation of the Anatolide belt, and that the crucial difference between the Hellenides and the Anatolides is due to along-strike variations in the Alpine subduction complex. In detail, aspects of the tectonic development of the Cycladic zone and the Anatolide belt will be reviewed, followed by a structural study of the Cycladic blueschist unit in western Turkey and the Menderes nappes. It will be shown that the tectonometamorphic differences of both units and the geometry of their thrust contact have significant implications on the timing of collision and exhumation processes, and on the palaeogeography of the eastern Mediterranean.

Overview

The nappe pile in the Aegean and western Turkey

The Hellenides can be subdivided from top (internides) to bottom (externides) into (1) the internal zone, (2) the Vardar–Izmir–Ankara zone, (3) the Lycian Allochthon, (4) the Cycladic zone, and (5) the external Hellenides (Fig. 2). A major difference between the Aegean and western Turkey is that in the latter the Menderes nappes instead of the external Hellenides form the lowermost tectonic unit (Fig. 2).

The internal zone consists of continental fragments of the Eurasian plate, the south-easternmost being the Sakarya continent (Fig. 1), underneath which oceanic crust of Neotethys was subducted during Cretaceous convergence (Şengör & Yilmaz 1981). The related suture is the Vardar–Izmir–Ankara zone (Şengör *et al.* 1984), parts of which were metamorphosed under blueschist-facies conditions in the Late Cretaceous (Sherlock *et al.* 1999) (Fig. 2c). The Lycian Allochthon (Collins & Robertson 1997) is a thin-skinned thrust belt, which roots in the Vardar–Izmir–Ankara zone (Collins & Robertson 1997, 1998, 1999). Within the Lycian Allochthon, top-to-the-south displacement occurred from the Late Cretaceous to the Late Miocene (Collins & Robertson 1998, 1999). Parts of the Lycian Allochthon were metamorphosed under incipient high-pressure conditions (Bernoulli *et al.* 1974; Franz & Okrusch 1992; Oberhänsli *et al.* 2001).

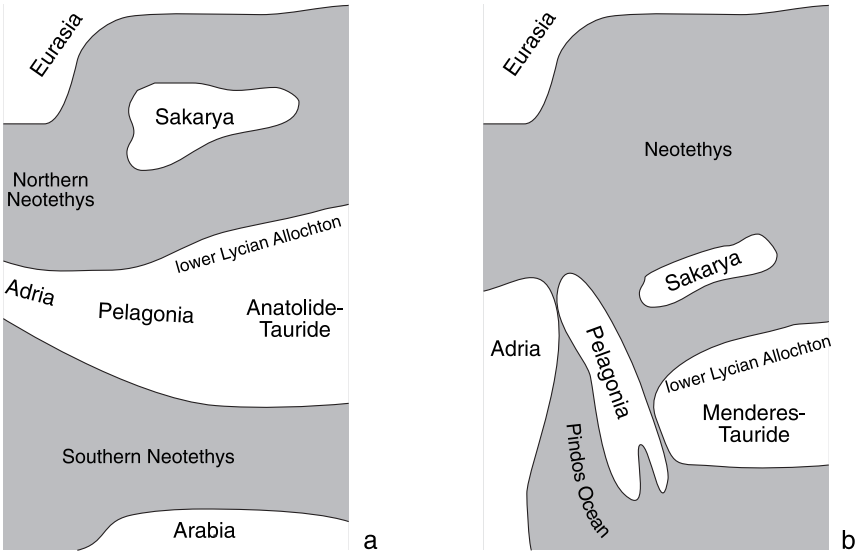

Fig. 1. Sketch maps of two common palaeogeographic models of the eastern Mediterranean illustrating the spatial arrangement of continents in the early Cretaceous modified from (**a**) Şengör & Yilmaz (1981) and (**b**) Robertson *et al.* (1996). Notice that in both models Pelagonia, Adria and the Anatolia (Menderes Tauride platform *sensu* Şengör & Yilmaz (1981); Anatolide–Tauride continent *sensu* Robertson *et al.* (1996)) represent the pre-Permian northern margin of Gondwana and that the lower Lycian Allochthon is assumed to represent part of the sedimentary cover of Anatolian Microcontinent.

The Cycladic zone consists of continental fragments of the Adriatic plate (Fig. 1) and can be subdivided into three tectonic units (Altherr & Seidel 1977; Avigad *et al.* 1997; Ring *et al.* 1999*b*), which are from structurally highest to lowest: (i) the heterogeneous Cycladic ophiolite nappe consisting of unmetamorphosed to greenschist-facies ophiolitic and sedimentary rocks containing high-grade metamorphic blocks of Jurassic and Cretaceous age. (ii) The Cycladic blueschist unit, which is made up of a high-pressure nappe stack comprising from top to bottom an ophiolitic mélange, a Permocarboniferous to Mesozoic shelf sequence, and a Carboniferous basement. (iii) The basal unit, which is exposed in at least four tectonic windows (Avigad *et al.* 1997; Ring *et al.* 2001*a*) (Fig. 2) and is likely to be part of the Permian to Palaeogene External Hellenides. Overall the temporal progradation of nappe emplacement and high-pressure metamorphism towards the south mimics the southward retreat of the Hellenic subduction zone.

In contrast to parts of the External Hellenides, the Menderes nappes, which also occur tectonically below the Cycladic zone, do not show Alpine high-pressure metamorphism (Ring *et al.* 1999*a*; Okay 2001). Another important difference is that the basement of one of the Menderes nappes (Çine nappe, see below) is of Neoproterozoic to Cambrian age (Kröner & Şengör 1990; Hetzel & Reischmann 1996; Hetzel *et al.* 1998; Loos & Reischmann 1999). This basement preserves deformation fabrics of latest Proterozoic age (the D_{PA} event of Gessner *et al.* 2001*a*; the suffix 'PA' stands for pre-Alpine). The absence of Alpine high-pressure metamorphism in the Menderes nappes and the lack of a well-defined subduction zone to the south of western Turkey suggest that subduction ceased after the collision of the exotic Anatolide microcontinent in the Eocene (Hetzel *et al.* 1995*b*; Ring *et al.* 1999*a*).

Lithology and tectonometamorphic evolution of the Cycladic blueschist unit in the Aegean

Aspects of the tectonometamorphic evolution of the Cycladic blueschist unit in the Aegean are reviewed here to allow comparisons with the development of the Cycladic blueschist unit in western Turkey. According to Ring *et al.* (1999*b*) the Cycladic blueschist unit on Samos Island consists of three high-pressure nappes, which are from top to bottom: (1) the Selçuk nappe (ophiolitic mélange), (2) the Ampelos nappe (Permocarboniferous to Mesozoic passive margin sequence), and (3) the Agios Nikolaos nappe (Carboniferous basement).

The Selçuk nappe contains blocks of metagabbro in a matrix of serpentinite and garnet–mica schist. Ring *et al.* (1999*b*) argued that the Selçuk nappe was correlative with the ophiolitic mélanges on the Cycladic islands of Syros and Tinos (Okrusch & Bröcker 1990; Bröcker & Enders 1999), where a rock unit similar in lithology and tectonic position is exposed. High-pressure *P–T* conditions are in the range of 10–15 kbar and 400–500°C (Ring *et al.* 1999*b*).

The Ampelos nappe and correlative tectonic units across the entire Cyclades consist of quartzite, metapelite and metabasite overlain by marble containing metabauxite (e.g. Dürr *et al.* 1978). This succession has been interpreted as a former passive continental margin sequence (Altherr & Seidel 1977). The underlying Agios Nikolaos nappe contains marble and garnet-mica schist intruded by Carboniferous orthogneiss, and represents part of the former basement of the shelf sequence. *P–T*

Fig. 2. Map, cross-sections and table showing the major tectonometamorphic units of the Hellenide-Anatolide orogenic belt and the southward progression of high-pressure metamorphism. The Pelagonian and Cycladic zones are shown together. The Cycladic blueschist unit makes up largest part of Cycladic zone, where it occurs below heterogeneous Cycladic ophiolite nappe and above post-middle Eocene metaflysch of External Hellenides. Windows of External Hellenides below Pelagonian and Cycladic zones are marked with asterisk and abbreviated OW, Olympus window; APW, Almyropotamos window; PW, Panormos window; KN, Kerketas nappe. Cross sections A–A' and B–B' show different units in footwall of Cycladic blueschist unit: External Hellenides in Aegean and Menderes nappes in western Turkey. Box indicates location of Figure 4. Modified after Schermer *et al.* (1990), Seidel *et al.* (1982), Avigad *et al.* (1997), Walcott (1998), Bröcker & Enders (1999) and Ring *et al.* (1999*b*). Insert shows location of main map in Mediterranean and regional extent of the Hellenides and Anatolides.

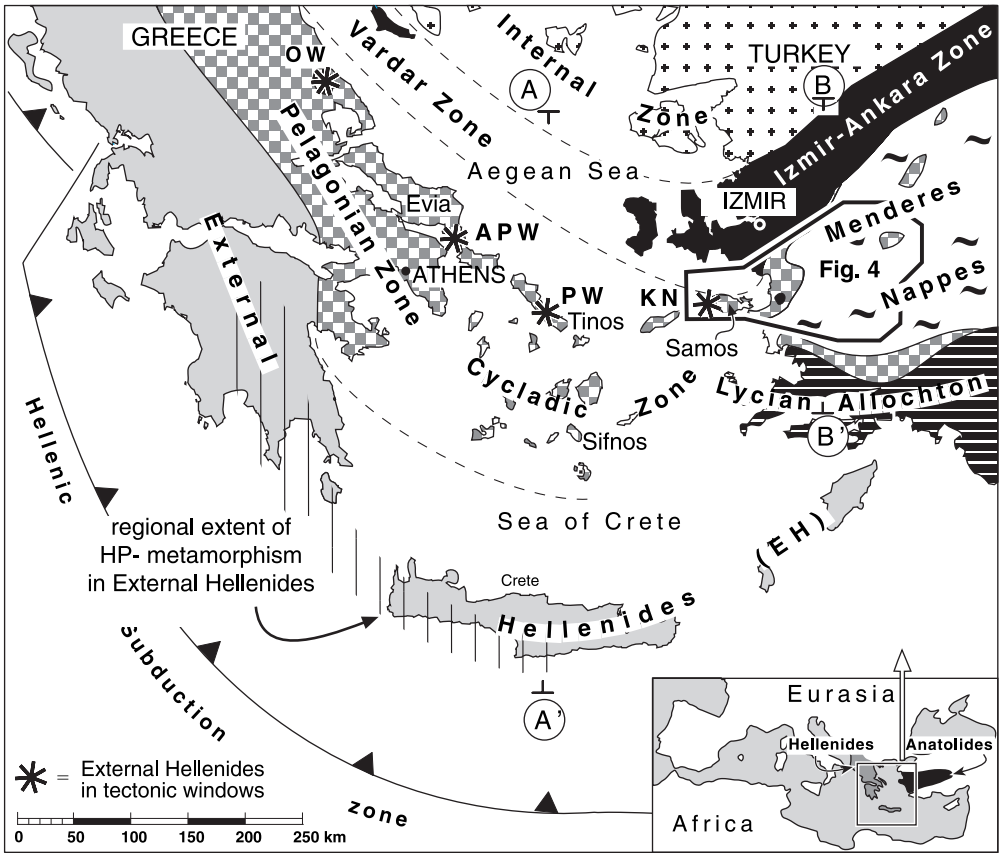

a

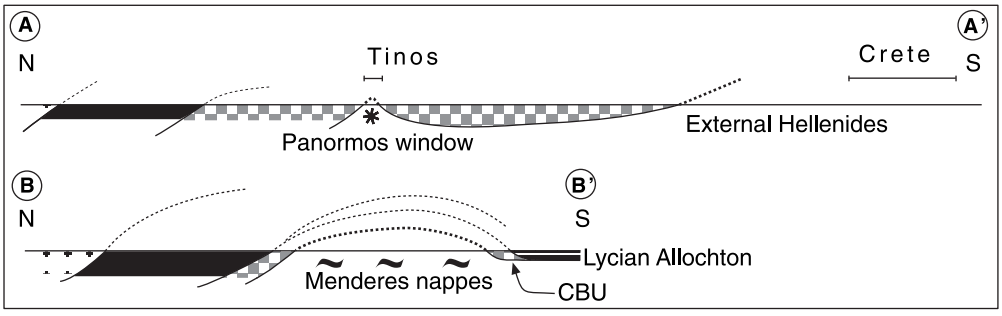

b

Tectonometamorphic unit subject to high–pressure metamorphism	Epoch: Cretaceous	Palaeocene	Eocene	Oligocene	Miocene	Time [Ma]	P / T [kbar/°C]	Authors
Vardar-Izmir-Ankara Zone	▮					~80	20 / 430	Sherlock et al. (1999)
Lycian Allochton	? ▮					?	7 / ~400	Franz & Okrusch (1992); Oberhänsli et al. (2000)
Cycladic zone (CZ)	▮					75-65	~12-19 / 450-550	Altherr et al. (1979); Wijbrans & McDougall (1986); Wijbrans et al. (1988; 1990); Bröcker et al. (1993); Bröcker & Enders (1999)
			▬			50-43		
✱ External Hellenides in tectonic windows in CZ					▬	24-20	8-10 / 400	Seidel et al. (1982); Ring et al. (2001)
HP in External Hellenides					▮	24-19	8-14 / 350-450	Theye & Seidel (1993); Thomson et al. (1999)

c

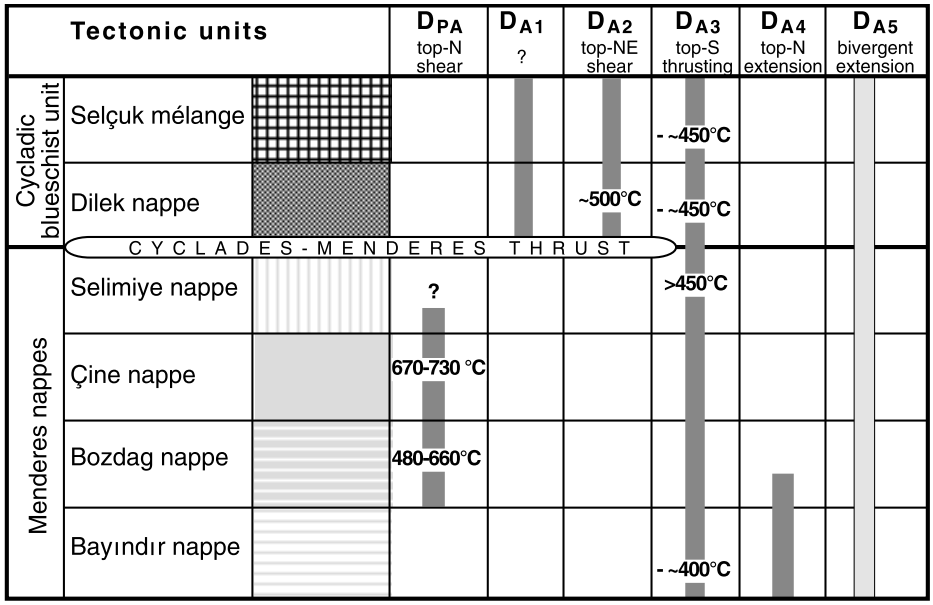

Fig. 3. Diagram showing distribution of pre-Alpine and Alpine events D_{PA} and D_{A1} to D_{A5} in the tectonic units of Anatolide belt. Temperature estimates after own observations, except for Çine and Bozdag nappes (Ring *et al.* in press) and Dilek nappe (Will *et al.* 1998). Diagram indicates that the Anatolide belt was assembled during D_{A3}. D_{A5} is outlined for its brittle deformation style; suffix 'PA' denotes pre-Alpine and 'A' Alpine deformation age.

conditions of the shelf/basement unit across the entire Cycladic zone are of the order of 12–19 kbar and 450–550°C (e.g., Okrusch & Bröcker 1990; Will *et al.* 1998).

The basal unit below the Cycladic blueschist unit largely consists of marbles capped by post-middle Eocene metaflysch. The basal unit underwent Oligocene to Miocene high-pressure metamorphism (Ring *et al.* 2001), which reached about 8–10 kbar and 350–400°C (Avigad *et al.* 1997; Ring *et al.* 1999*b*). A subsequent Barrovian metamorphism overprinted all high-pressure units and reached greenschist- to amphibolite-facies conditions.

Age data for high-pressure metamorphism show a consistent pattern across the Aegean. Zircons, which had overgrown high-pressure minerals in the ophiolitic mélanges of Syros and Tinos were dated by the U–Pb method at 78 Ma and 63–61 Ma (Bröcker & Enders 1999). High-pressure metamorphism in the underlying shelf/basement unit is usually placed into the Eocene (53–40 Ma) and cooling during decompression below *c.*350–400°C took place between 40 and 35 Ma (e.g. K/Ar, $^{40}Ar/^{39}Ar$, and Rb–Sr white mica ages of Altherr *et al.* 1979; Maluski *et al.* 1987 and Bröcker *et al.* 1993). The Barrovian-type overprint occurred at about 25–15 Ma (e.g. Altherr *et al.* 1979, 1982; Wijbrans & McDougall 1986, 1988; Wijbrans *et al.* 1990; Bröcker *et al.* 1993). High-pressure rocks of the basal unit date from *c.* 40 to 35 Ma in the Olympus window (Schermer *et al.* 1990), from 24 to 21 Ma on Evia and Samos (Ring *et al.* 2001) and 24 to 20 Ma in Crete (Seidel *et al.* 1982; Thomson *et al.* 1999).

The tectonometamorphic evolution of the Cycladic blueschist unit in the Aegean involved structures formed during prograde high-pressure metamorphism. The structures young structurally downwards and were poikiloblastically overgrown by glaucophane, chloritoid and kyanite (Lister & Raouzaios 1996 for Sifnos Island; Ring *et al.* 1999*b* for Samos Island). During subsequent decompression, thrusting of the Cycladic blueschist unit onto the basal unit was associated with moderate high-pressure metamorphism in the latter (Avigad *et al.* 1997; Ring *et al.* 1999*b*; Ring *et al.* 2001). Succeeding mid-Oligocene to Recent crustal-scale extension occurred before, during and after the Barrovian metamorphic event. Extension is manifest by greenschist-facies shear zones and brittle normal faults, which are inferred to represent different generations of detachment systems (Forster & Lister 1999; Ring *et al.* 2001).

The exhumation of the Cycladic blueschist unit is generally attributed to middle Oligocene normal faulting caused by rollback of the subducting Hellenic slab (e.g. Lister *et al.* 1984; Buick 1991; Raouzaios *et al.* 1996). Avigad *et al.* (1997) and Ring *et al.* (1999*b*), however, argued that on the islands of Evia and Samos up to 30–40 km of the exhumation of the Cycladic blueschist unit occurred before the middle Oligocene.

Lithology and tectonometamorphic evolution of the Menderes nappes

Three Alpine deformation events, abbreviated D_{A3}–D_{A5} (suffix 'A' indicates an Alpine age), have been recognized in the Menderes nappes (the Alpine deformation events D_{A1} and D_{A2} are only found in the Cycladic blueschist unit, see below). Some of the Menderes nappes were affected by a pre-Alpine event (D_{PA}; Fig. 3) (Gessner *et al.* 2001). The Menderes nappes consist from top to bottom of (1) the Selimiye nappe, (2) the Çine nappe, (3) the Bozdag nappe and (4) the Bayındır nappe (Ring *et al.* 1999*a*; Gessner *et al.* 2001*a*) (Figs 4 and 5).

The Selimiye nappe contains a metasedimentary sequence, the basal part of which is of Precambrian age (Hetzel & Reischmann 1996; Loos & Reischmann 1999). Preliminary structural work suggests that an amphibolite-facies fabric of as yet unresolved kinematics and age was overprinted by the Alpine D_{A3} top-to-the-south Selimiye shear zone, which separates the Selimiye nappe from the underlying Çine nappe. The Selimiye shear zone formed during prograde greenschist-facies metamorphism and related structures were overgrown by garnet at temperatures >450°C (Hetzel & Reischmann 1996). Hetzel & Reischmann (1996) showed that $^{39}Ar/^{40}Ar$ muscovite ages of 43–37 Ma record slow cooling below 350–400°C (assumed closure temperature for Ar diffusion in muscovite) after D_{A3} and after garnet growth.

The Çine and Bozdag nappes are characterized by a distinct overprinting sequence of ductile fabrics. The structurally higher Çine nappe consists of amphibolite to granulite-facies

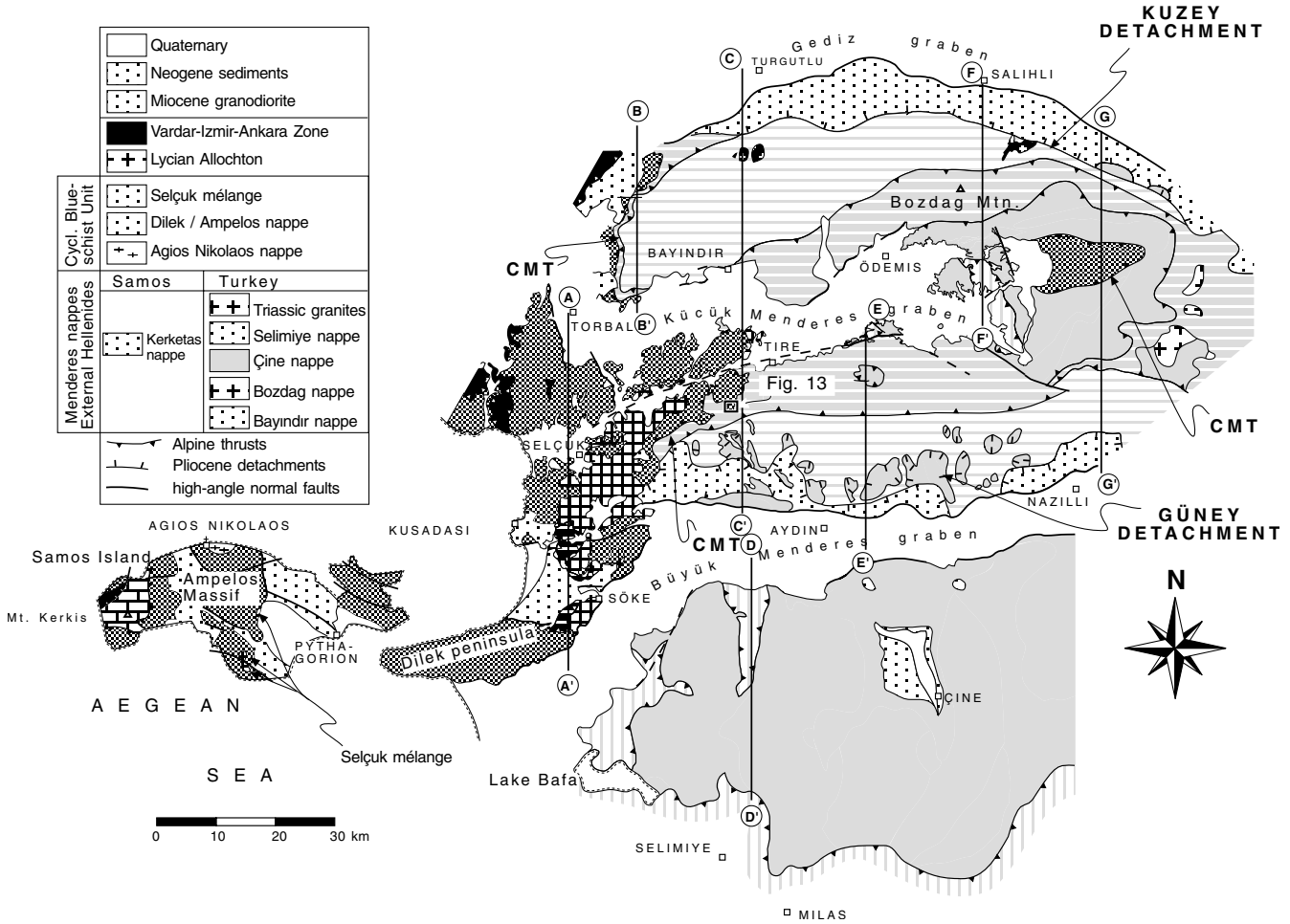

Fig. 4. Tectonic map of western Turkey and Samos Island after Hetzel *et al.* (1995*b*), Hetzel (1995*a*), Dora *et al.* (1995), Candan & Dora (1998), Güngör (1998), Ring *et al.* (1999*a*), Ring *et al.* (1999*b*) and own observations. Lines for cross sections A–A′ to G–G′ (Fig. 5) and location of Figure 12 are indicated; CMT, Cyclades–Menderes thrust.

ortho- and paragneiss with intercalated metabasite (Dora *et al.* 1995; Lackmann 1997), while the Bozdag nappe is composed of amphibolite-facies garnet–mica schist and metabasite. Gessner *et al.* (2001) gave geochronological evidence that the D_{PA} event in the Bozdag and Çine nappes occurred during amphibolite-facies metamorphism at *c.* 550 Ma and caused top-to-the-NE shear. D_{PA} was overprinted by a D_{A3} greenschist-facies tectonometamorphic event. The corresponding S_{A3} foliation crosscuts S_{PA} and produced a variably spaced shear-band foliation and a well-defined stretching lineation associated with top-to-the-south kinematic indicators in both nappes and also in Triassic metagranite (cf. Fig. 4) (Gessner *et al.* 2001*a*). Exact *P–T* conditions for Alpine greenschist-facies metamorphism during D_{A3} are unknown.

The Bayındır nappe at the base contains shelf sediments of inferred Permo-Carboniferous age (Osman Candan pers. comm. 1998), which were metamorphosed under lower greenschist-facies conditions at *c.*37 Ma (Lips *et al.* 2001). The absence of biotite in rocks of suitable bulk composition suggests temperatures $\leq c.400$°C (Yardley 1989). The Bayındır nappe was deformed by the synmetamorphic D_{A3} event, which is the first deformation event in the Bayındır nappe. The corresponding S_{A3} foliation is penetrative and associated with a fine-grained N-trending stretching lineation (L_{A3}) (Fig. 6b). L_{A3} is expressed by stretched quartz, albite and chlorite aggregates and aligned tourmaline. In the structurally highest parts of the Bayındır nappe north of Aydın, D_{A3} ductile shear bands and sigma-type objects (Passchier & Simpson 1986) indicate a top-to-the-south shear sense. However, north of Bozdag Mountain, mylonite that formed during the intrusion of the middle Miocene Turgutlu and Salihli granodiorites (Fig. 4), shows consistent top-to-the-north shear sense indicators associated with ductile extensional deformation (Hetzel *et al.* 1995*b*). Because the structures north of Bozdag Mountain formed in the middle Miocene, they are about 15–20 million years younger than the D_{A3} fabrics, which formed during greenschist-facies metamorphism at *c.*37 Ma (Lips *et al.* 2001). Therefore, the structures north of Bozdag Mountain are likely to represent a separate D_{A4} ductile extensional event.

Late Alpine brittle extension (D_{A5}) is expressed by normal-fault systems of Miocene to Recent age (Cohen *et al.* 1995; Hetzel *et al.* 1995*a*; Emre & Sözbilir 1997). Since the Pliocene, two opposite-facing normal-fault systems, the Kuzey detachment in the north and the Güney detachment in the south (Ring *et al.* 1999*a*), have evolved into rolling hinges and have produced the synclinal structure of the Central Menderes

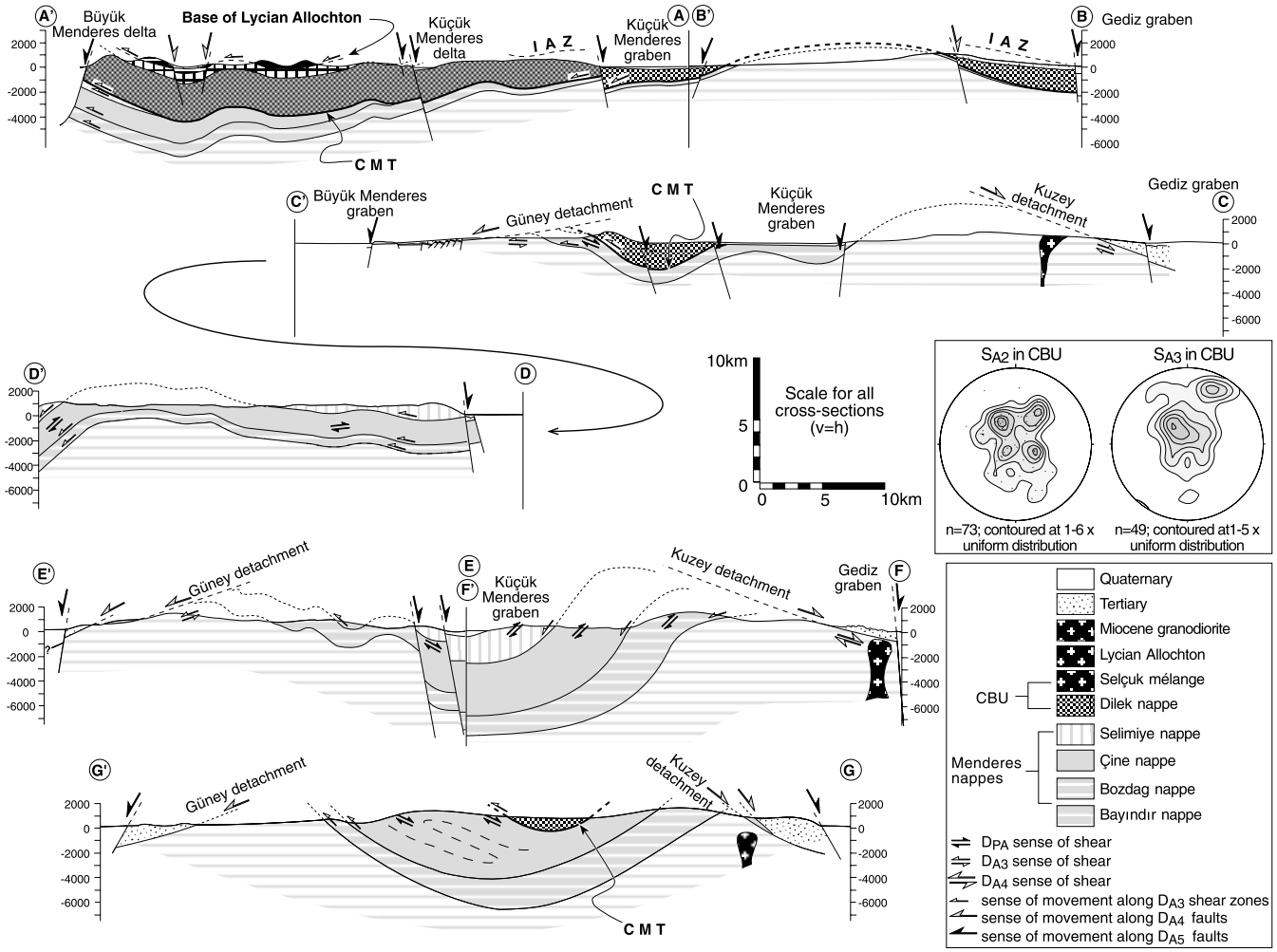

Fig. 5. Cross sections A–A' to G–G' (position of sections given in Fig. 4). Section A–A' shows that Cyclades–Menderes thrust cuts up-section towards the south in direction of tectonic transport. For geometric viability section planes are oriented parallel to mean orientation of L_{A3}. Trace of foliation is projected into section plane and used to infer geometry of sub-surface structures.

metamorphic core complex (Gessner *et al.* 2001*b*) (Figs 4 and 5).

Overall, this summary reveals two important aspects: (1) there is no evidence for Alpine high-pressure metamorphism in the Menderes nappes and (2) the available, albeit scarce data suggest that grade and age of metamorphism associated with D_{A3} decrease structurally downward. Temperatures in the Selimiye nappe were >450°C and occurred before 43–37 Ma (Hetzel & Reischmann 1996), whereas in the Bayındır nappe temperatures barely reached 400°C and occurred later at *c.* 37 Ma (Lips *et al.* 2001).

The Cycladic blueschist unit in western Turkey

Lithology and metamorphism

In western Turkey the Cycladic blueschist unit is made up by the Selçuk mélange and the underlying Dilek nappe (Erdogan & Güngör 1992; Candan *et al.* 1997; Güngör 1998; Ring *et al.* 1999*a*). The Selçuk mélange consists of blocks of metagabbro and metabauxite-bearing marble, which are surrounded by a matrix of serpentinite and garnet-mica schist. The Dilek nappe is a metamorphosed Permo-Mesozoic shelf sequence, which includes a quartzite conglomerate with interlayered kyanite-chloritoid schist, metabasite, phyllite and marble containing metabauxite. Deposition age of the marble ranges from late Triassic through middle Palaeocene (Dürr *et al.* 1978; Özer *et al.* 2001). The passive-margin sequence is overlain by lower to middle Palaeocene flysch (Özer *et al.* 2001). The Selçuk mélange correlates with the Selçuk nappe; the Dilek nappe is correlative with the Ampelos nappe in Samos (Candan *et al.* 1997; Ring *et al.* 1999*a*). No Carboniferous basement is exposed below the Dilek nappe in western Turkey.

Candan *et al.* (1997) reported *P–T* conditions of >10 kbar and <470°C for high-pressure metamorphism in the Dilek nappe, which approximates the *c.*15 kbar and 500°C estimated for the Ampelos nappe on Samos (Will *et al.* 1998). $^{39}Ar/^{40}Ar$ ages for phengite were interpreted to date high-pressure metamorphism at *c.* 40 Ma in the Dilek nappe (Oberhänsli *et al.* 1998). $^{39}Ar/^{40}Ar$ work by Ring *et al.* (unpublished data) on Samos Island suggests that ages of *c.*37–40 Ma reflect phengite recrystallization during a high-pressure deformation event, which post-dated the peak of high-pressure metamorphism.

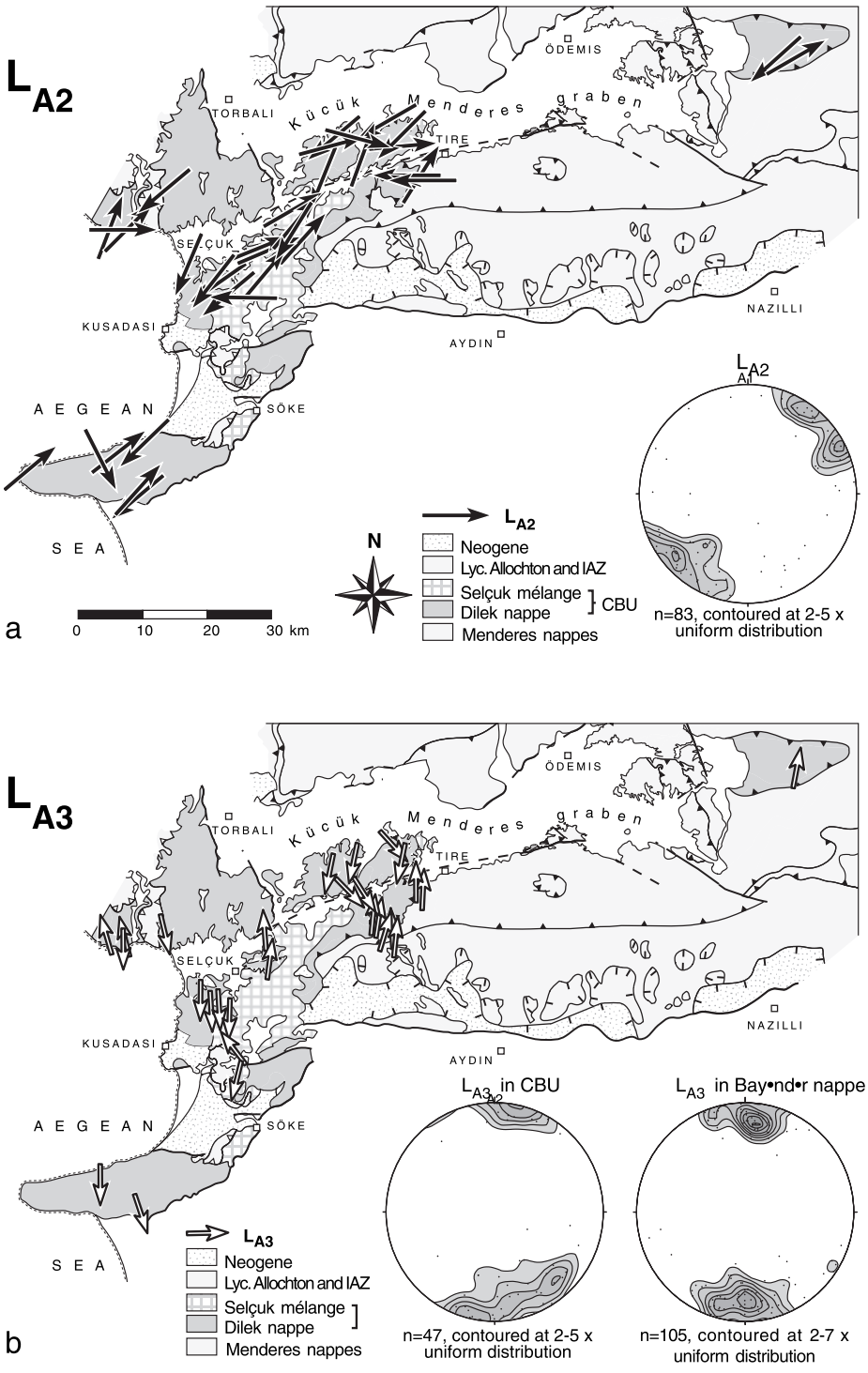

Fig. 6. Orientations of stretching lineations L_{A2} (a) and L_{A3} (b) in map view and stereograms (equal-area lower-hemisphere projections). In (b), a stereogram of L_{A3} in Bayındır nappe is shown for comparison.

Deformation history

Given the Late Cretaceous fossil evidence in the Dilek nappe, deformation events in the Cycladic blueschist unit in western Turkey must be of Alpine age, and will accordingly be abbreviated D_{A1}, D_{A2} and D_{A3}. D_{A1} fabric elements occur exclusively as microscopic relics in the Dilek nappe; mesoscopic D_{A2} and D_{A3} fabrics are present in both the Selçuk mélange and the Dilek nappe.

D_{A1} is limited to the internal foliation S_{A1} in millimetre- to centimetre-sized chloritoid and kyanite porphyroclasts in the Dilek nappe (Fig. 7a–c). In some porphyroclasts, a diffuse opaque banding oriented at a small angle to S_{A1} may represent a sedimentary or a pre-D_{A1} deformation fabric (Fig. 7b).

A second foliation S_{A2} developed heterogeneously in rocks of the Selçuk mélange. Serpentinite and metapelite display a penetrative foliation, which is associated with a well-defined

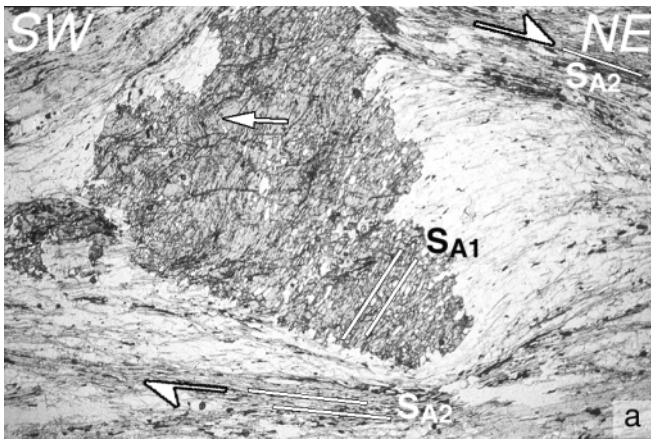

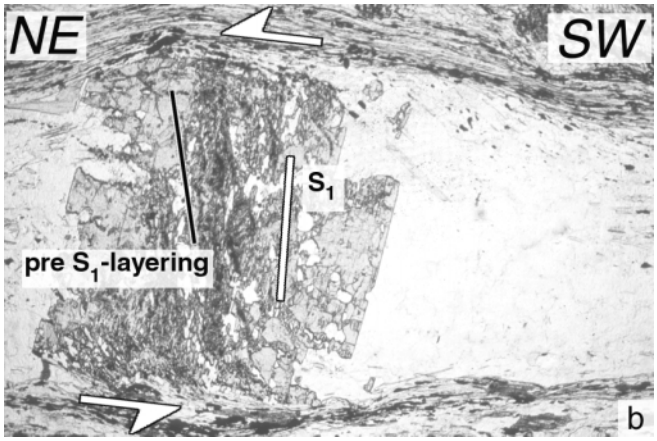

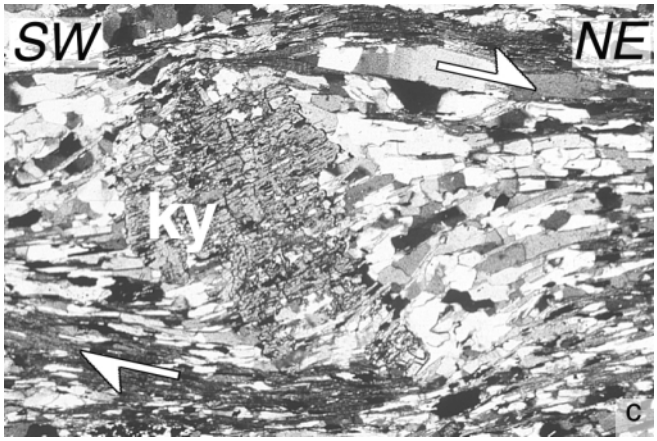

Fig. 7. Relation between foliations S_{A1} and S_{A2} and the inferred sense of shear in kyanite-chloritoid schist intercalations in quartzite conglomerate of the Dilek nappe. Mineral abbreviations: ky, kyanite; cld, chloritoid). Location of outcrop: 37°54.24N, 027°21.92E. (**a**) Chloritoid σ-type porphyroclast (*sensu* Passchier & Simpson 1986) with the internal foliation S_{A1} oriented at a high angle to S_{A2} in the matrix. Notice that crenulation of opaque banding is indicated by arrow. Sense of shear is top-to-the-NE. Plane polarized light, field of view is 13 × 18 mm. (**b**) Chloritoid porphyroclast with curved inclusion trails illustrating angular relationship between pre-S_{A1} opaque banding, internal foliation S_{A1}, and foliation S_{A2} in matrix. Sense of shear is top-to-the-NE. Plane polarized light, field of view is 9 × 13.5 mm. (**c**) Kyanite porphyroclast with σ-type geometry indicating top-to-the-NE sense of shear. Field of view is 1.8 × 2.7 mm.

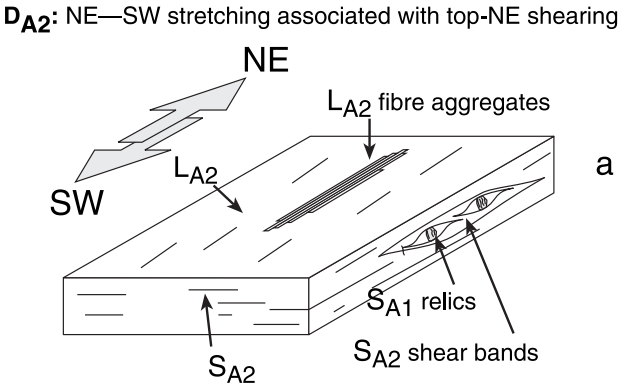

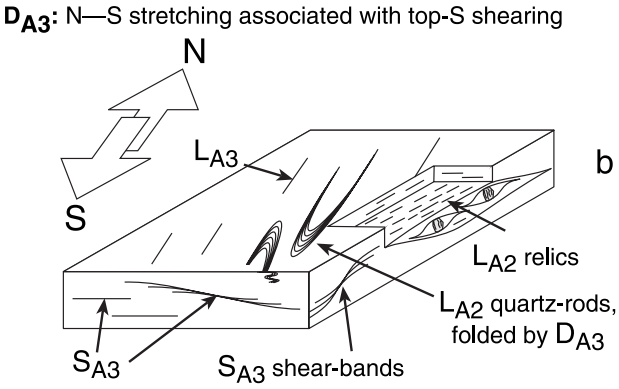

Fig. 8. Cartoon illustrating different regional stretching directions during (**a**) D_{A2} and (**b**) D_{A3} defined by mean orientations of L_{A2} and L_{A3}; notice the D_{A1} relics in kyanite-chloritoid schist layers within lenses of quartz conglomerate.

NE- to east-trending stretching lineation. Some metabasic and ultrabasic lithologies occur as massive, largely unfoliated blocks. In the Dilek nappe, D_{A2} fabrics are best preserved in marble, quartzite and kyanite-chloritoid schist, whereas in phyllite only relics of D_{A2} occur. In quartzite and marble, the arrangement of quartz, calcite, white mica and chlorite defines a pervasive S_{A2} foliation parallel to lithological layering. In kyanite-chloritoid schist, S_{A2} is the dominant foliation, which is expressed by the preferred orientation of white mica and flattened quartz. On S_{A2}, a stretching lineation L_{A2} is expressed by elongated quartz pebbles and quartz-fibre aggregates in quartzite, kyanite–chloritoid schist and phyllite and by elongated aggregates of white mica in marble. Stretched L_{A2} quartz-fibre aggregates commonly occur as folded rods or in microlithons between later S_{A3} shear bands. Locally, kyanite laths, epidote and blue amphibole are aligned subparallel to L_{A2}. In zones where a D_{A3} fabric is weak or absent, L_{A2} generally trends NE (Fig. 6a), whereas in zones of high D_{A3} strain, the orientation of L_{A2} scatters around the north direction.

In zones of high D_{A3} strain, L_{A2} was apparently aligned subparallel to L_{A3}. The present difference of *c.* 45° between the azimuths of the L_{A2} and L_{A3} stretching lineations in rocks which are not or only weakly deformed by D_{A3} is probably close to the original angular separation between L_{A2} and L_{A3}

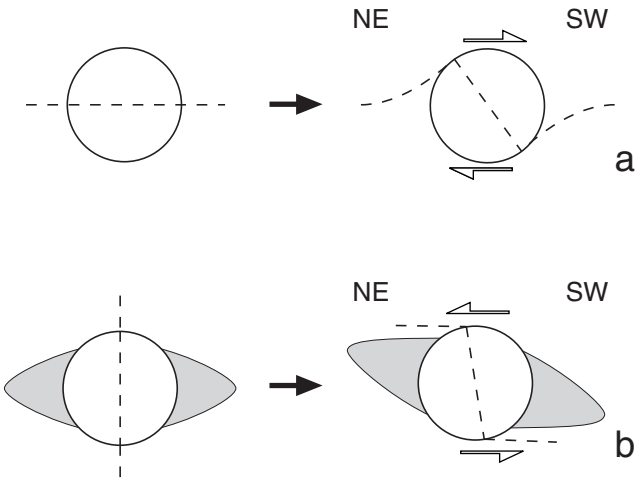

Fig. 9. Schematic model for the development of porphyroclasts. (**a**) The porphyroclast rotates freely with respect to flow eigenvectors; internal and external foliation in this case belong to same generation (i.e. S_{A2}) and the inferred sense of shear would be dextral, i.e. top-to-the-SW. (**b**) Case, in which the foliation rotates sinistrally (i.e. top-to-the-NE) with respect to the porphyroclast which largely remains stationary because it is coupled with strain shadows. Because foliation rotates relative to porphyroclast new cleavage domains (S_{A2}) form between strain shadows. Case (b) is preferred, because it agrees with sense of shear indicated by shear bands in matrix. Notice that steep dip of internal foliation in porphyroclast is likely to be close to original attitude of S_{A1}.

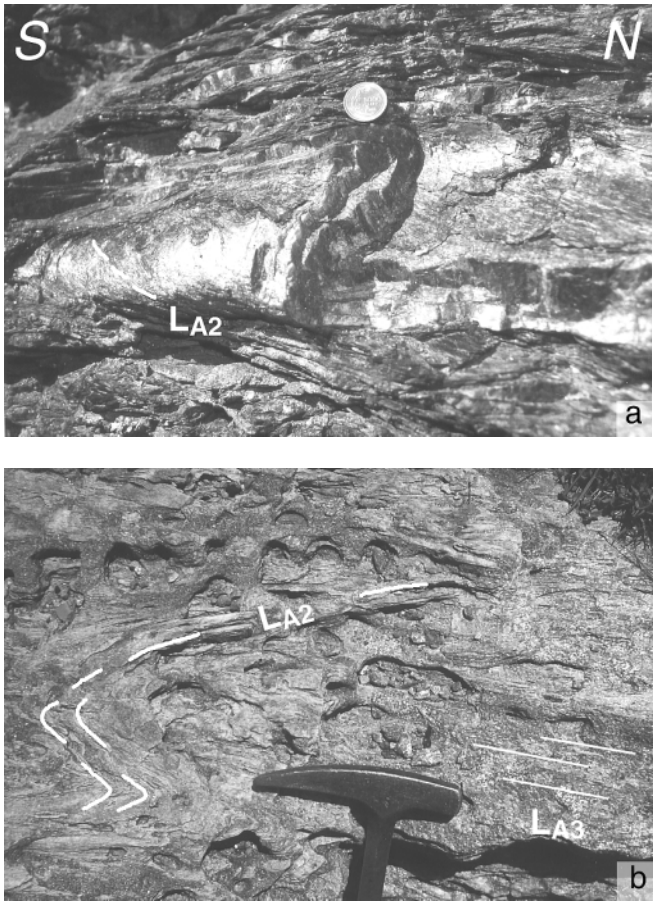

Fig. 10. Outcrop photographs of D_{A2} fabrics. (**a**) Folding of S_{A2} and L_{A2} about N-trending F_{A3} fold axes in calcschist-phyllite intercalation. Location of outcrop 37°54.24N, 027°21.92E. (**b**) Sheath folding of L_{A2} quartz rod in albite–epidote greenschist of Dilek nappe. L_{A3} is expressed by north-trending fine-grained white-mica-aggregate lineation; plan view, outcrop is located at 38°00.76N 027°06.23E.

(Fig. 8a, b). The original orientation of L_{A2} can therefore be assumed to have been about NE–SW.

Shear sense associated with D_{A2} is not obvious in the outcrops, but a consistent top-to-the-NE sense of shear can be detected at the microscopic scale in kyanite–chloritoid schists. These contain σ-shaped objects made up of chloritoid and kyanite porphyroclasts with strain shadows containing recrystallized quartz (Fig. 7a, c). The asymmetries displayed by the external and internal foliations of kyanite and chloritoid porphyroclasts can be explained by two kinematic models which yield opposite shear sense (Passchier & Trouw 1996, fig. 7.34a) (Fig. 9a and b). In the first model (Fig. 9a), the asymmetries are caused by dextral (i.e. top-to-the-SW in our specific case) rotation of the clast with respect to the flow eigenvectors and the external foliation. In the second model (Fig. 9b), the external foliation rotates sinistrally (i.e. top-to-the-NE) with respect to the flow eigenvectors, while the clast is rotating little or not at all because it is coupled with the strain shadows. The latter model applies to the kyanite and chloritoid porphyroclasts described here, because of the asymmetric, stair-stepping shape of the strain shadows. Moreover, the top-to-the-NE displacement along shear bands in the matrix independently point to the same conclusion.

The contact between the Selçuk mélange and the Dilek nappe is exposed west of Tire. There, garnet–mica schist of the Selçuk mélange overlies kyanite-bearing calcschist of the Dilek nappe. At the contact, D_{A2} structures are pervasive. S_{A2} layering is parallel to the contact and is associated with NE-trending L_{A2}, defined by stretched calcite–mica aggregates and up to 30 mm long kyanite laths.

D_{A3} structures deformed the D_{A2} fabrics in the Selçuk mélange and the Dilek nappe. These overprinting relations and differences in structural style allow for a distinction between D_{A2} and D_{A3} fabrics in many places. D_{A3} is well-documented in phyllite and greenschist of the Dilek nappe whereas, in the Selçuk mélange, D_{A3} structures are rare. S_{A3} occurs as a penetrative cleavage in phyllosilicate-rich lithologies, in which S_{A2} is strongly transposed and S_{A3} usually forms the dominant foliation. In marble and quartzite, S_{A3} is mostly absent. In composite lithologies like phyllite-quartzite alternations and calcschist, S_{A3} represents a heterogeneous shear-band foliation, in which D_{A2} fabrics are offset by S_{A3} shear bands. In microlithons between the S_{A3} shear bands, crenulation of S_{A2} is frequently observed. A north-trending L_{A3} stretching lineation (Fig. 6b) is expressed by fine-grained white mica-chlorite-quartz aggregates. In zones of high D_{A3} strain, folding of S_{A2} and L_{A2} is common with F_{A3} axes oriented subparallel to L_{A3} (Fig. 10a) and locally L_{A2} quartz rods are folded into F_{A3} sheath folds (Fig. 10b). Macroscopic kinematic indicators associated with D_{A3} fabrics in the Dilek nappe display a uniform top-to-the-south shear sense (Fig. 11a, b).

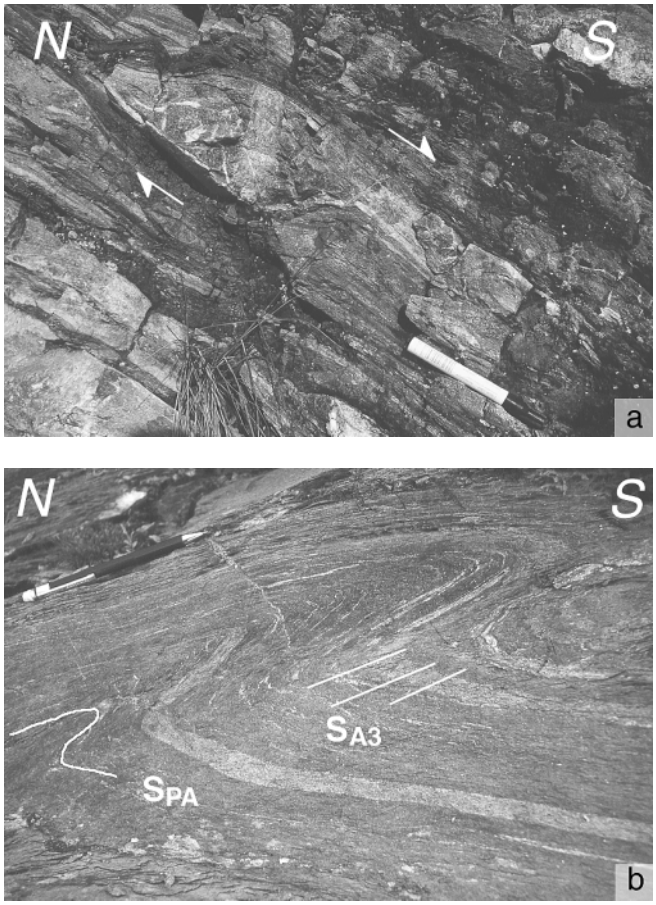

Fig. 11. Macroscopic D_{A3} shear-sense indicators. (**a**) D_{A3} shear zone in calcschist of Dilek nappe with σ-type object of marble indicating top-to-the-S sense of shear; location is 37°55.01′N, 027°20.12′E. (**b**) Asymmetric D_{A3} fold in quartzite of Bozdag nappe with closely spaced axial-planar S_{A3} cleavage. Outcrop is located at 38°01.75′N, 27°41.11′E.

The Cyclades–Menderes thrust

The Cyclades–Menderes thrust cuts through several nappes of the underlying Menderes nappe pile (Figs 4 and 5). In the Selçuk–Tire region, the Cyclades–Menderes thrust separates the Dilek nappe from the Bozdag nappe. East of Ödemis, the Dilek nappe overlies para- and orthogneiss of the Çine nappe. South of Selimiye, the Cyclades–Menderes thrust is obscured by a series of imbrications, but most likely separates the Dilek nappe from the Selimiye nappe.

The Cyclades–Menderes thrust has been studied in detail in the Selçuk–Tire region, where it is well exposed along a ridge crest NW of Yemisler (Fig. 12). There, the base of the Dilek nappe consists of quartzite and marble, which make up the twin peaks Ballikkayası Tepe and Bozkaya Tepesi. The southern slope of the ridge consists of garnet-mica schist and amphibolite of the Bozdag nappe in the footwall of the Cyclades–Menderes thrust. South of Yemisler, amphibolite-facies D_{PA} structures dominate the fabric in the Bozdag nappe. The S_{PA} foliation is expressed by flattened potassium feldspar and quartz and by preferred orientation of white mica and biotite. S_{PA} is associated with a NE-trending L_{PA} stretching lineation made up by elongated biotite-white mica and quartz-potassium feldspar aggregates. Shear bands indicate a top-to-the-NE sense of shear. In a several hundred metres thick section north of the village of Yemisler, the amphibolite-facies D_{PA} structures in the Bozdag nappe are progressively destroyed within a greenschist-facies shear zone (Fig. 13a, b). Overprinting criteria, style and metamorphic grade of the foliation and fold axes, as well as the orientation of the stretching lineation (cf. Fig. 11) and associated kinematic indicators allow the correlation of these greenschist-facies structures with D_{A3} structures in the overlying Dilek nappe.

Interpretation of deformation–metamorphism–timing relationships

D_{A1} and D_{A2}

Chloritoid and kyanite form a peak high-pressure assemblage in the Ampelos nappe in Samos (Will *et al.* 1998) and the correlative Dilek nappe in western Turkey. The temporal relation between the formation of S_{A1} and S_{A2} and the growth of chloritoid and kyanite reveals aspects of the tectonometamorphic history of the Dilek nappe during high-pressure metamorphism. An interpretative sequence of the relationship between the development of structures and mineral growth is shown in Figure 14a–d. Growth of chloritoid and kyanite porphyroblasts occurred after the formation of S_{A1} and overlapped with the onset of D_{A2} structures. Early during D_{A2}, chloritoid and kyanite ceased to grow (Fig. 14c), which makes a relation of D_{A2} to decompression likely. $^{40}Ar/^{39}Ar$ phengite age data obtained by Ring *et al.* (unpublished) for Samos Island suggest an age of *c.* 40 Ma for D_{A2}.

D_{A3}

Deformation–metamorphism relations during D_{A3} are complex and heterogeneous. In the Selimiye nappe, Hetzel & Reischmann (1996) reported growth of garnet (i.e. temperatures exceeding 450°C) after the formation of the D_{A3} Selimiye shear zone. Accordingly, $^{40}Ar/^{39}Ar$ white-mica ages from the Selimiye shear zone were interpreted to date cooling after shearing (Hetzel & Reischmann 1996). In the Bayındır nappe at the base of the Menderes nappes, D_{A3} fabrics formed at peak-metamorphic temperatures of $\leq$400°C (Fig. 3). Hence, the $^{40}Ar/^{39}Ar$ white-mica ages of Lips (2001) closely date D_{A3} in the Bayındır nappe. As suggested above, downward propagation of D_{A3} thrusting was associated with decreasing temperatures.

Deformation–metamorphism relations across the Cyclades–Menderes thrust indicate that the breakdown of garnet and biotite to chlorite in the Bozdag nappe at temperatures $\leq c.$400°C (Yardley 1989) occurred during D_{A3} mylonitization. As temperatures during deformation along the Cyclades–Menderes thrust appear to have been at least 50°C lower than in the Selimiye shear zone and the inverted metamorphic gradient in the Menderes nappe pile may be older than the Cyclades–Menderes thrust. It therefore appears reasonable to regard the Cyclades–Menderes thrust as a late D_{A3} structure. In concert with geometric constraints (Figs 5 and 15), the age data suggest that the emplacement of the Cycladic blueschist unit was by out-of-sequence thrusting.

Discussion

Tectonic implications

Detailed structural work across the contact of the Dilek nappe with the underlying Bozdag nappe reveals that this contact is a

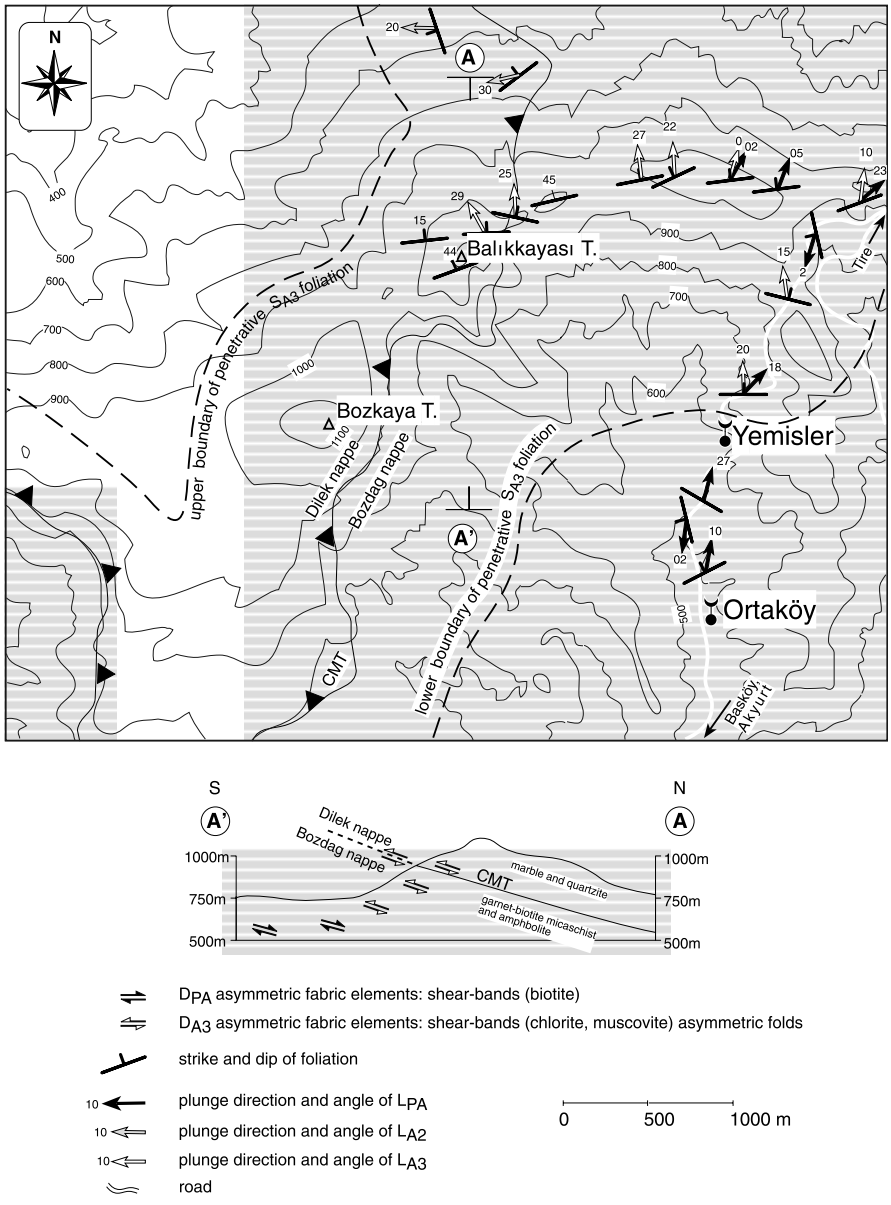

Fig. 12. Structural map and cross section from area southwest of Tire, where the Cyclades-Menderes Thrust is exposed (box in Fig. 4 shows location of map). The dashed line indicates the extent of D_{A3} fabrics across the Cyclades–Menderes thrust.

late D_{A3} greenschist-facies shear zone, the Cyclades–Menderes thrust, along which the Cycladic blueschist unit was emplaced on top of the Menderes nappes by out-of-sequence thrusting. Significant differences in tectonometamorphic history of the hanging wall and footwall prior to movement along the Cyclades–Menderes thrust imply large displacements along the latter. In the Cycladic blueschist, the Cyclades–Menderes thrust overprinted a two-phase Alpine high-pressure history; in the footwall, the Cyclades–Menderes thrust crosscuts pre-Alpine structures. During mylonitization along the Cyclades–Menderes thrust the temperature was relatively low at least in the upper portion of the Menderes nappe pile, if compared to the temperature at which D_{A3} fabrics formed in the Selimiye nappe. This suggests that the Menderes nappes had been assembled early during D_{A3}, before the Cycladic blueschist unit was emplaced.

The reason for proposing that D_{A3} and the associated Cyclades–Menderes thrust resulted from crustal shortening is that the Cycladic blueschist unit ramped upwards relative to the Earth's surface in the direction of D_{A3} transport. As illustrated in Figure 5, the Cyclades–Menderes thrust cuts up-section through the Menderes nappe pile, which was assembled during an earlier stage of D_{A3}. Within the Menderes nappes, the inverted metamorphic gradient also suggests crustal shortening. Even if the original dip of the Menderes nappe contacts had been subhorizontal, the Cyclades-Menderes thrust still would have had to be somewhat steeper in order to cut up-section in the direction of transport. This geometry is displayed in Figure 15, which illustrates the proposed thrust sequence and the thermochronological data. The mylonitic rocks in the Selimiye shear zone cooled below 350–400°C between 43 and 37 Ma (Hetzel & Reischmann 1996) (thrust 5 in Fig. 15). D_{A3} thrusting in the Menderes nappes progressed structurally downwards and affected the Bayındır nappe at *c.*37 Ma (Lips 2001) (thrusts 6 and 7 in Fig. 15). If this interpretation is correct, phengite $^{40}Ar/^{39}Ar$ ages of 40 Ma reported by Oberhänsli *et al.* (1998) from the Dilek nappe would overlap with the cooling ages below the Cyclades–Menderes thrust. This implies that greenschist-facies displacement of the Cycladic blueschist unit along the

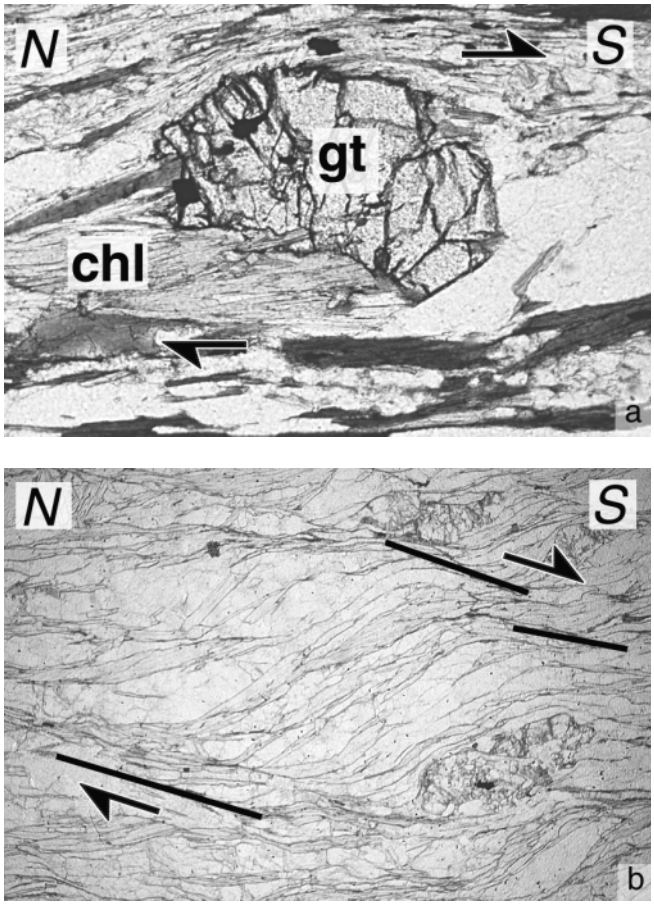

Fig. 13. Microstructures across the Cyclades–Menderes thrust. (**a**) Photomicrograph showing retrograde growth of chlorite (chl) at the expense of garnet (gt) in garnet-biotite schist of the Bozdag nappe. Asymmetric tails of chlorite indicate top-to-south directed shearing during retrogression; plane polarized light, field of view 3.5 × 5.3 mm, location of outcrop 38°01.94N, 27°41.22E. (**b**) Photomicrograph of quartzite mylonite of the Dilek nappe in the hanging wall of the Cyclades–Menderes thrust with shear bands showing top-to-the-south displacement; plane polarized light, field of view 11 × 16 mm, location of outcrop is 38°02.59N, 27°40.58E.

Cyclades–Menderes thrust occurred shortly after the end of blueschist-facies metamorphism; D_{A2} and D_{A3} in part might even have overlapped in time. It remains unclear whether deformation of the Bayındır nappe occurred before, during or after motion at the Cyclades–Menderes thrust. Further thermochronological research is needed to better constrain the age of the Cyclades–Menderes thrust.

Overall, the tectonic evolution in western Turkey as outlined in Figure 15 is in striking contrast to the orogenic development in the Aegean, where the Cycladic blueschist unit rests on the External Hellenides. The latter show early Oligocene high-pressure metamorphism in tectonic windows and early Miocene high-pressure metamorphism in Crete and the Peleponnesos (Fig. 2). The downward propagating high-pressure metamorphism in the Aegean was probably controlled by progressive southward retreat of the Hellenic subduction zone, which most likely commenced in the Eocene (Thomson *et al.* 1998). In western Turkey, subduction-zone retreat was probably halted when the exotic Anatolide microcontinent (Fig. 16) entered the subduction zone in the Eocene (Hetzel *et al.* 1995*a*; Ring *et al.* 1999*a*). We speculate that the overall continental architecture of Anatolia was different from that of easternmost Adria. While the crust of the latter was thinned and maybe even oceanic (Pindos Basin), and had probably been easier to subduct than the crust of Anatolia there is no indication that the crust of Anatolia was thinned at all before entering the subduction zone; it therefore successfully resisted deep subduction (Fig. 16). Wijbrans & McDougall (1988) made a similar proposition by suggesting that the Cycladic zone had formerly been a collage of small fragments of easily subductable continental crust. We speculate that accretion of Anatolia caused early D_{A3} thrusting in the upper Menderes nappes (thrusts 5 and 6 in Fig. 15). Accretion of the Bayındır nappe may have caused a change in the geometry of the orogenic wedge, hence triggering additional shortening, back-stepping of thrusting towards the hinterland and out-of-sequence emplacement of the Cycladic blueschist unit onto the Menderes nappes. This model allows simultaneous in-sequence motion of the Bozdag nappe onto the Bayındır nappe and out-of-sequence movement at the Cyclades–Menderes thrust. Given the scarce thermochronological data, the proposed thrust sequence remains speculative but provides a testable working hypothesis.

The observation that the Cycladic blueschist unit sits on top of the Menderes nappes has also implications for the Lycian Allochthon above the Cycladic blueschist unit. Because orogenic development progressed structurally downward, high-pressure metamorphism in the Lycian Allochthon should be older than that in the Cycladic blueschist unit (i.e. pre 40 Ma). Such an inference fits well into the recently proposed tectonic model for the Lycian Allochthon by Collins & Robertson (1998, 1999). However, the tectonic position of the Lycian Allochthon above the ophiolitic Selçuk mélange implies that the lower units of the Lycian Allochthon were either deposited on a promontory of Adria or Sakarya ('Lycia' in Fig. 16), or on a separate continental fragment rather than being part of Anatolia, as is generally assumed (cf. Fig. 1) (Sengör & Yilmaz 1981; Sengör *et al.* 1984; Collins & Robertson 1998).

Exhumation of the Cycladic blueschist unit

The overgrowth of S_{A1} by a blueschist-facies mineral assemblage suggests that D_{A1} occurred during prograde high-pressure metamorphism and is probably related to nappe stacking in the Cycladic blueschist unit (see Lister & Raouzaios (1996) for Sifnos Island and Ring *et al.* (1999*b*) for Samos Island). The subsequent D_{A2} event occurred during initial decompression, i.e., exhumation, and may have reactivated the nappe contact of the Dilek nappe and the Selçuk mélange. If the age of 40 Ma produced by Oberhänsli *et al.* (1998) represents phengite crystallization, the Cycladic blueschist unit in Turkey must have been rapidly exhumed by *c.* 35 km before its greenschist-facies emplacement onto the Menderes nappes during late D_{A3} at about 37 Ma (Lips *et al.* 2001). How this pronounced exhumation was accomplished is largely unknown. Avigad *et al.* (1997, fig. 13) inferred an Oligocene extensional event for Tinos; Ring *et al.* (1999*b*) estimated 30–40 km of Eocene to early Oligocene exhumation of the Cycladic blueschist unit by vertical ductile thinning and erosion for Samos.

There are two possible tectonic interpretations of D_{A2} top-to-the-NE shear. (1) D_{A2} is related to back thrusting of the Cycladic blueschist unit onto its hinterland due to the

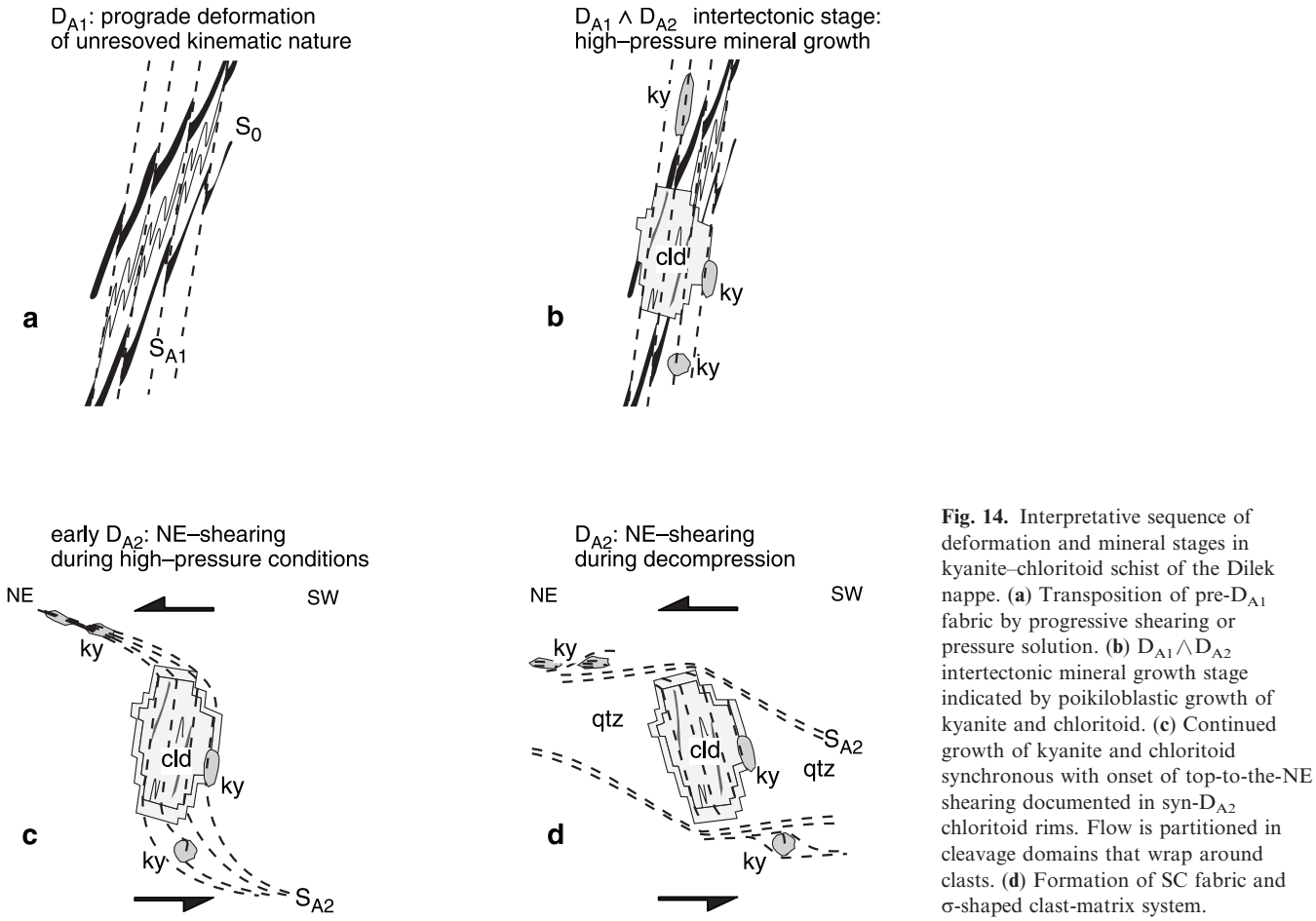

Fig. 14. Interpretative sequence of deformation and mineral stages in kyanite–chloritoid schist of the Dilek nappe. (**a**) Transposition of pre-D_{A1} fabric by progressive shearing or pressure solution. (**b**) $D_{A1} \wedge D_{A2}$ intertectonic mineral growth stage indicated by poikiloblastic growth of kyanite and chloritoid. (**c**) Continued growth of kyanite and chloritoid synchronous with onset of top-to-the-NE shearing documented in syn-D_{A2} chloritoid rims. Flow is partitioned in cleavage domains that wrap around clasts. (**d**) Formation of SC fabric and σ-shaped clast-matrix system.

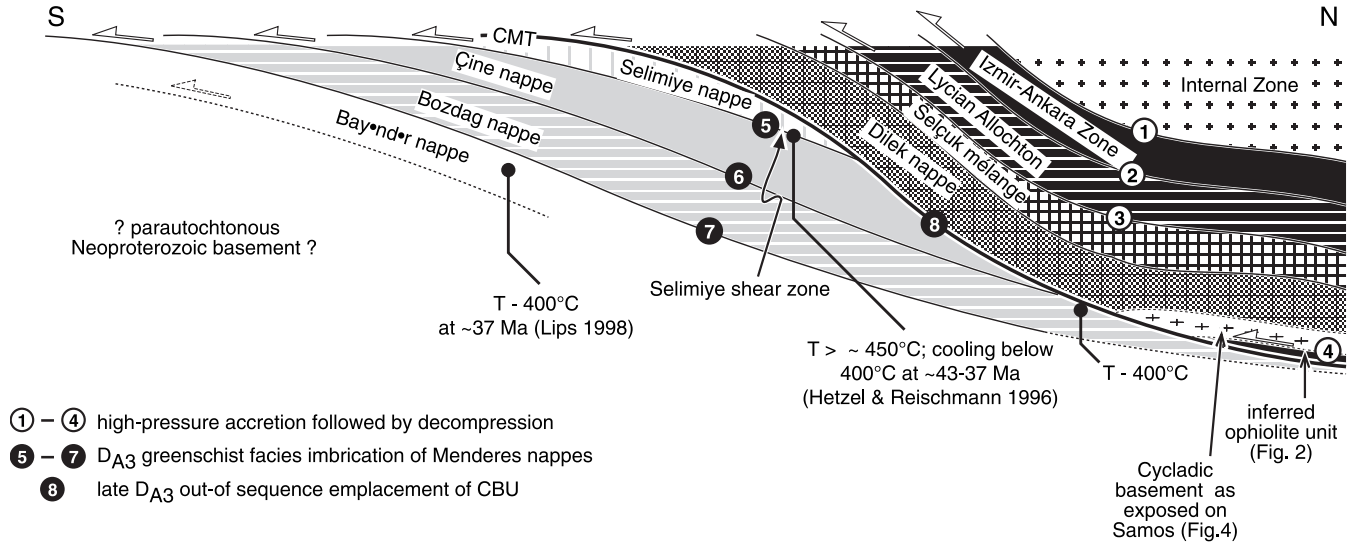

Fig. 15. Interpretative thrust sequence during formation of Anatolide belt. Late Cretaceous to early Eocene imbrication of Vardar–Izmir–Ankara suture zone and Cycladic blueschist unit during high-pressure metamorphism (thrusts 1–4), followed by collision of Anatolia causing greenschist-facies imbrication within Menderes nappes (thrusts 5–7).

development of topographic gradients in the accretionary wedge (e.g., Willett *et al.* 1993). Accordingly, S_{A2} should have originally dipped towards the SW, but pervasive D_{A3} shearing may have rotated S_{A2} into subparallelism with the north-dipping penetrative S_{A3} foliation. The *c.*35 km of exhumation would then be due to vertical ductile thinning and erosion. (2) D_{A2} is related to normal faulting, which aided exhumation of the Cycladic blueschist unit during D_{A2} in the Eocene. An initially high angle between S_{A1} and the instantaneous stretching axis of D_{A2} can be inferred from S_{A1} and S_{A2} in those

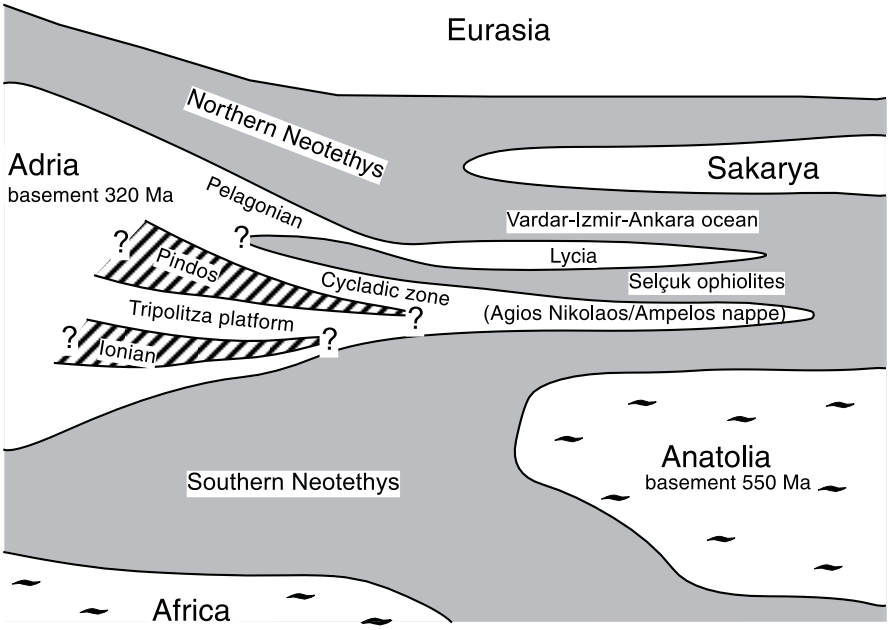

Fig. 16. Palaeogeographic sketch map for early Cretaceous modified from Sengör & Yilmaz (1981) and Robertson *et al.* (1996) illustrating the spatial arrangement of continents and continental fragments and their basement ages. Adria is shown to taper toward the east; its crust is in part highly thinned as indicated by Ionian and Pindos zones; the latter of which may in part have been oceanic. Anatolia is interpreted as a microcontinent which had rifted from Africa in the early Mesozoic and, unlike Adria, consisted of 'normal' thickness continental crust.

porphyroclasts which retained their initial position between the strain shadows during shearing (Fig. 9). The high angle between S_{A1} and S_{A2} may reflect a pronounced change of the flow field, i.e., a strain reversal, and would lend strong support into an extensional interpretation of D_{A2}. If D_{A2} reworked the contact between the Dilek nappe and the Selçuk mélange, the Dilek nappe should have decompressed faster in the Eocene than the Selçuk mélange. Further work is needed to resolve this issue, which may have significance for exhumation processes in the eastern Mediterranean.

Conclusions

The Anatolide belt of western Turkey was assembled by top-to-the-south thrusting of the Cycladic blueschist unit onto the Menderes nappes during greenschist-facies metamorphism in the Eocene. The Menderes nappes as part of the Anatolian microcontinent successfully resisted subduction, whereas the easternmost part of the Adriatic plate had been subject to sustained high-pressure metamorphism. The different tectonometamorphic history of these units contradicts the model that the Menderes nappes are the eastern continuation of the Cycladic blueschist unit. The Cycladic blueschist unit displays a prograde Alpine D_{A1} fabric, which was overgrown by a high-pressure mineral assemblage. The onset of D_{A2} occurred during initial decompression after this high-pressure event and is associated with top-to-the-NE shearing. A subsequent top-to-the-south greenschist-facies D_{A3} event affected the Cycladic blueschist unit and the Menderes nappes together. Late during D_{A3} the contact between the Cycladic blueschist unit and the Menderes nappes, the Cyclades–Menderes thrust, formed. The Cyclades–Menderes thrust defines an out-of sequence ramp structure, which cuts up-section through Menderes nappes towards the south. In the Cycladic blueschist unit, late D_{A3} fabrics associated with the Cyclades-Menderes thrust crosscut high-pressure D_{A2} structures. In the footwall, D_{PA} structures in the Bozdag nappe were deformed by the Cyclades–Menderes thrust. The Cycladic blueschist unit was exhumed by *c.* 35 km before the Cyclades–Menderes thrust formed in the Eocene. D_{A2} structures aided this early exhumation, either by vertical ductile thinning, normal faulting, or a combination of both.

Funded by the Deutsche Forschungsgemeinschaft (grants Ri 538/4-1, 538/4-2 and 538/4-3 and Graduiertenkolleg 392, 'Stoffbestand und Entwicklung von Kruste und Mantel'). We thank J. M. Bartley and A. C. Collins for constructive reviews.

References

Altherr, R. & Seidel, E. 1977. Speculations on the geodynamic evolution of the Attic-Cycladic crystalline complex during alpidic times. *In:* Kallergis, G. (ed.) *Geology of the Aegean region, Proceedings VI Colloquium, Athens*. Institute of Geology and Mineral Exploration, 347–351.

Altherr, R., Schliestedt, M., Okrusch, M., Seidel, E., Kreuzer, H., Harre, W., Lenz, H., Wendt, I. & Wagner, G. A. 1979. Geochronology of high-pressure rocks on Sifnos (Cyclades, Greece). *Contributions to Mineralogy and Petrology*, **70**, 245–255.

Altherr, R., Kreuzer, H., Wendt, I., Lenz, H., Wagner, G. H., Keller, J., Harre, W. & Höhndorf, A. 1982. A late Oligocene/early Miocene high temperature belt in the Attic-Cycladic crystalline complex (SE Pelagonian, Greece). *Geologisches Jahrbuch*, **E23**, 97–164.

Aubouin, J. 1959. Contribution a l'étude de la Grèce septrionale; les confins de l'Epire et de la Thessalie. *Annales géologiques des Pays Hellèniques*, **10**, 1–483.

Avigad, D., Garfunkel, Z., Jolivet, J. & Azañón, J. M. 1997. Back arc extension and denudation of Mediterranean eclogites. *Tectonics*, **16**, 924–941.

Bernoulli, D., Graciansky, P. C. D. & Monod, O. 1974. The Extension of the Lycian nappes (SW Turkey) into the southeastern Aegean islands. *Eclogae Geologicae Helveticae*, **67**, 39–90.

Bröcker, M., Kreuzer, H., Matthews, A. & Okrusch, M. 1993. $^{40}Ar/^{39}Ar$ and oxygen isotope studies of polymetamorphism from Tinos Island, Cycladic blueschist belt, Greece. *Journal of metamorphic Geology*, **11**, 223–240.

Bröcker, M. & Enders, M. 1999. U–Pb zircon geochronology of unusual eclogite-facies rocks from Syros and Tinos (Cyclades, Greece). *Geological Magazine*, **136**, 111–118.

Brunn, J. H. 1956. Contribution a l'étude géologique du Pinde septentrional et d'une partie de la Macédonie Occidentale. *Annales géologiques des Pays Hellèniques*, **7**, 1–358.

Buick, I. S. 1991. The late-Alpine evolution of an extensional shear zone, Naxos, Greece. *Journal of the Geological Society of London*, **152**, 639–654.

CANDAN, O., DORA, O. O., OBERHÄNSLI, R., CETINKAPLAN, M., PARTZSCH, J. H., WARKUS, F. C. & DÜRR, S. 1997. Blueschist relics in the Mesozoic cover series of the Menders Massif and correlations with Samos Island, Cyclades. *Schweizerische Mineralogische und Petrographische Mitteilungen*, **77**, 95–99.

CANDAN, O. & DORA, O. O. 1998. *The generalized map of the Menderes Massif*. Jeoloji Mühendisligi Bölümü Dokuz Eylül University Bornova, Izmir.

COHEN, H. A., DART, C. J., AKYÜZ, H. S. & BARKA, A. 1995. Syn-rift sedimentation and structural development of the Gediz and Büyük Menderes graben, western Turkey. *Journal of the Geological Society, London*, **152**, 629–638.

COLLINS, A. S. & ROBERTSON, A. H. F. 1997. Lycian mélange, southwest Turkey: An emplaced Cretaceous accretionary complex. *Geology*, **25**, 255–258.

COLLINS, A. S. & ROBERTSON, A. H. F. 1998. Process of Late Cretaceous to Late Miocene episodic thrust-sheet translation in the Lycian Taurides. *Journal of the Geological Society, London*, **155**, 759–772.

COLLINS, A. S. & ROBERTSON, A. H. F. 1999. Evolution of the Lycian Allochthon, western Turkey, as a north-facing Late Palaeozoic to Mesozoic rift and passive continental margin. *Geological Journal*, **34**, 107–138.

DORA, O. O., CANDAN, O., DÜRR, S. H. & OBERHÄNSLI, R. 1995. New evidence of the geotectonic evolution of the Menderes Massif *In: Proceedings of the International Earth Sciences Colloquium on the Aegean Region*. Güllük, Turkey.

DÜRR, S. H., ALTHERR, R., KELLER, J., OKRUSCH, M. & SEIDEL, E. 1978. The Median Aegean Crystalline belt: stratigraphy, structure, metamorphism, magmatism. *In:* CLOOS, H., ROEDER, D. & SCHMIDT, K. (eds) *Alps, Appenines, Hellenides*. Schweitzerbart, Stuttgart, 455–477.

EMRE, T. & SÖZBILIR, H. 1997. Field evidence for metamorphic core complex, detachment faulting and accomodation faults in the Gediz and Büyük Menderes Grabens, Western Anatolia *In: Proceedings of the International Earth Sciences Colloquium on the Aegean Region*. Güllük, Turkey, **1**, 73–94.

ERDOGAN, B. & GÜNGÖR, T. 1992. Stratigraphy and tectonic evolution of the northern Margin of the Menderes Massif. *Bulletin of the Turkish Association of Petroleum Geologists*, **4**, 9–34.

FORSTER, M. A. & LISTER, G. S. 1999. Detachment faults in the Aegean core complex of Ios, Cyclades, Greece. In RING, U., BRANDON, M.T., LISTER, G.S. & WILLETT, S.D. (eds) *Exhumation Processes: Normal Faulting, Ductile Flow and Erosion*. Geological Society, London. Special Publications, **154**, 305–323.

FRANZ, L. & OKRUSCH, M. 1992. Aragonite-bearing blueschists on Arki Island, Dodecanese, Greece. *European Journal of Mineralogy*, **4**, 527–537.

GESSNER, K., PIAZOLO, S., GÜNGÖR, T., RING, U., KRÖNER, A. & PASSCHIER, C. W. 2001*a*. Tectonic significance of deformation patterns in granitoid rocks of the Menderes nappes, Anatolide belt, southwest Turkey. *International Journal of Earth Sciences (Geologische Rundschau)*, **89**, 766–780.

GESSNER, K., JOHNSON, C., RING, U., GÜNGÖR, T. & PASSCHIER, C. W. 2001*b*. An active bivergent rolling-hinge detachment system: The Central Menderes metamorphic core complex in western Turkey. *Geology*, **29**, 611–614.

GÜNGÖR, T. 1998. *Stratigraphy and tectonic evolution of the Menderes Massif in the Söke-Selçuk Region*. PhD thesis. Dokuz Eylül University, Izmir.

HETZEL, R. & REISCHMANN, T. 1996. Intrusion age of Pan-African augen gneisses in the southern Menderes massif and the age of cooling after Alpine ductile extensional deformation. *Geological Magazine*, **133**, 565–572.

HETZEL, R., PASSCHIER, C. W., RING, U. & DORA, O. O. 1995*a*. Bivergent extension in orogenic belts: the Menderes massif, southwestern Turkey. *Geology*, **23**, 455–458.

HETZEL, R., RING, U., AKAL, C. & TROESCH, M. 1995*b*. Miocene NNE-directed extensional unroofing in the Menderes massif, southwestern Turkey. *Journal of the Geological Society of London*, **152**, 639–654.

HETZEL, R., ROMER, R. L., CANDAN, O. & PASSCHIER, C. W. 1998. Geology of the Bozdag area, central Menderes massif, SW-Turkey: Pan African basement and Alpine deformation. *Geologische Rundschau*, **87**, 394–380.

JACOBSHAGEN, V. 1986. *Geologie von Griechenland*. Borntraeger, Berlin.

JACOBSHAGEN, V., DUERR, S., KOCKEL, F. KOPP, K. O., KOWALCZYK, G., BERCKHEMER, H. & BUETTNER, D. 1978. Structure and geodynamic evolution of the Aegean region. *In:* CLOOS, H. *ET AL.* (eds) *Alps, Apennines, Hellenides*. Inter-Union Commission on Geodynamics Scientific Report, **38**, 537–564.

KRÖNER, A. & SENGÖR, A. M. C. 1990. Archean and Proterozoic ancestry in late Precambrian to early Proterozoic crustal elements of southern Turkey as revealed by single-zircon dating. *Geology*, **18**, 1186–1190.

LACKMANN, W. 1997. *P-T Entwicklung von Metapeliten des zentralen Menderes Massivs, Türkei*. Diploma thesis. Johannes Gutenberg-Universität Mainz.

LIPS, A. L. W., CASSARD, D., SÖZBILIR, H., YILMAZ, H. & WIJBRANS, J. R. 2001. Multistage exhumation of the Menderes Massif, western Anatolia (Turkey). *International Journal of Earth Sciences (Geologische Rundschau)*, **89**, 781–792.

LISTER, G. S., BANGA, G. & FEENSTRA, A. 1984. Metamorphic core complexes of Cordilleran type in the Cyclades, Aegean Sea, Greece. *Geology*, **12**, 221–225.

LISTER, G. S. & RAOUZAIOS, A. 1996. The tectonic significance of a porphyroblastic blueschist facies overprint during Alpine orogenesis, Sifnos, Aegean Sea, Greece. *Journal of Structural Geology*, **18**, 1417–1435.

LOOS, S. & REISCHMANN, T. 1999. The Evolution of the southern Menderes Massif in SW Turkey as revealed by zircon dating. *Journal of the Geological Society, London*, **156**, 1021–1030.

MALUSKI, H., BONNEAU, M. & KIENAST, J. R. 1987. Dating the metamorphic events in the Cycladic area: $^{39}Ar/^{40}Ar$ data from metamorphic rocks of the island of Syros (Greece). *Bulletin de la Société géologique de France*, **8**, 833–842.

OBERHÄNSLI, R., MONIÉ, P., CANDAN, O., WARKUS, F. C., PARTZSCH, J. & DORA, O. O. 1998. The age of blueschist metamorphism in the Mesozoic cover series of the Menderes Massif. *Schweizerische Mineralogische und Petrographische Mitteilungen*, **78**, 309–316.

OBERHÄNSLI, R., PARTZSCH, J. H., CANDAN, O. & CETINKAPLAN, M. 2001. First occurrence of Fe-Mg-carpholite documenting a High Pressure metamorphism in metasediments of the Lycian Nappes, SW Turkey. *International Journal of Earth Sciences (Geologische Rundschau)*, **89**, 867–873.

OZER, S., SÖZBILIR, H., OZKAR, I., TOKER, V. & SARI, B. 2001. Stratigraphy of Upper Cretaceous-Palaeogene sequences in the southern and eastern Menderes Massif (western Turkey). *International Journal of Earth Sciences (Geologische Rundschau)*, **89**, 852–866.

OKAY, A. I. 2001. Stratigraphic and metamorphic inversions in the central Menderes Massif: a new structural model. *International Journal of Earth Sciences (Geologische Rundschau)*, **89**, 709–727.

OKRUSCH, M. & BRÖCKER, M. 1990. Eclogite facies rocks in the Cycladic blueschist belt, Greece: A review. *European Journal of Mineralogy*, **2**, 451–478.

PARÉJAS, E. 1940. La tectonique transversale de la Turquie. *Reviews of the Faculty of Science of the University of Istanbul Series B*, **5**, 133–244.

PASSCHIER, C. W. & SIMPSON, C. 1986. Porphyroclast systems as kinematic indicators. *Journal of Structural Geology*, **8**, 831–844.

PASSCHIER, C. W. & TROUW, R. A. W. 1996. *Microtectonics*. Springer, Berlin.

RAOUZAIOS, A., LISTER, G. S. & FOSTER, D. A. 1996. Oligocene exhumation and metamorphism of eclogite-blueschists from the island Sifnos, Cyclades, Greece. *Geological Society of Australia Abstracts*, **41**, 358.

RING, U., GESSNER, K., GÜNGÖR, T. & PASSCHIER, C. W. 1999*a*. The Menderes Massif of western Turkey and the Cycladic Massif in the Aegean—do they really correlate?. *Journal of the Geological Society, London*, **156**, 3–6.

RING, U., LAWS, S. & BERNET, M. 1999*b*. Structural analysis of a complex nappe sequence and late orogenic basins from the Aegean Island of Samos, Greece. *Journal of Structural Geology*, **21**, 1575–1602.

RING, U., LAYER, P. W. & REISCHMANN, T. 2001. Miocene high-pressure metamorphism in the Cyclades and Crete, Aegean Sea, Greece: Evidence for large-magnitude displacement on the Cretan detachment. *Geology*, **29**, 395–398.

RING, U., WILLNER, A. & LACKMANN, W. Nappe stacking and clockwise versus anticlockwise pressure-temperature paths: an example from the Menderes nappes of western Turkey. *American Journal of Science*, in press.

ROBERTSON, A. H. F. & DIXON, J. E. 1984. Introduction: aspects of the geological evolution of the eastern Mediterranean. *In:* DIXON, J. E. & ROBERTSON, A. H. F. (EDS) *The Geological Evolution of the Eastern Mediterrean*. Geological Society, London. Special Publications, **17**, 1–74.

ROBERTSON, A. H. F., DIXON, J. E., BROWN, S., COLLINS, A. S., MORRIS, A., PICKETT, E., SHARP, I. & USTAÖMER, T. 1996. Alternative tectonic models for the Late Palaeozoic–Early Tertiary development of Tethys in the Eastern Mediterranean region. *In:* MORRIS, A. & TARLING, D.H. (eds) *Palaeomagnetism and Tectonics of the Mediterranean Region*. Geological Society, London. Special Publications, **105**, 239–263.

SCHERMER, E. R., LUX, D. R. & BURCHFIEL, B. C. 1990. Temperature-time history of subducted continental crust, Mount Olympos Region, Greece. *Tectonics*, **9**, 1165–1196.

SEIDEL, E., KREUZER, H. & HARRE, W. 1982. A late Oligocene/early Miocene high pressure belt in the External Hellenides. *Geologisches Jahrbuch*, **E 23**, 165–206.

ŞENGÖR, A. M. C. & YILMAZ, Y. 1981. Tethyan Evolution of Turkey: a plate tectonic approach. *Tectonophysics*, **75**, 181–241.

ŞENGÖR, A. M. C., SATIR, M. & AKKÖK, R. 1984. Timing of the tectonic events in the Menderes massif, western Turkey: implications for tectonic evolution and evidence for Pan-African basement in Turkey. *Tectonics*, **3**, 693–707.

SHERLOCK, S., KELLEY, S., INGER, S., HARRIS, N. & OKAY, A. 1999. ^{40}Ar-^{39}Ar and Rb-Sr geochronology of high-pressure metamorphism and exhumation history of the Tavsanli Zone, NW Turkey. *Contributions to Mineralogy and Petrology*, **137**, 46–58.

THEYE, T. & SEIDEL, E. 1993. Uplift-related retrogression history of aragonite marbles in Western Crete (Greece). *Contributions to Mineralogy and Petrology*, **114**, 349–356.

THOMSON, S. N., STÖCKHERT, B., RAUCHE, H. & BRIX, M. R. 1998. Apatite fission-track thermochronology of the uppermost tectonic unit of Crete, Greece: implications for the post-Eocene tectonic evolution of the Hellenic subduction system. *In:* VAN DEN HAUTE, P. & DE CORTE, F. (eds) *Advances in Fission-Track Geochronology*. Kluwer Academic, Dordrecht, 187–205.

THOMSON, S. N., STÖCKHERT, B. & BRIX, M. R. 1999. Miocene high-pressure metamorphic rocks of Crete, Greece: rapid exhumation by buoyant escape. *In:* RING, U., BRANDON, M.T., LISTER, G.S. & WILLETT, S.D. (eds) *Exhumation Processes: Normal Faulting, Ductile Flow and Erosion*. Geological Society, London. Special Publications, **154**, 87–107.

WALCOTT, C. R. 1998. The Alpine evolution of Thessaly (NW) Greece and late Tertiary Aegean kinematics. *Geologica Ultraiectina*, **162**, 1–175.

WIJBRANS, J. R. & MCDOUGALL, I. 1986. $^{40}Ar/^{39}Ar$ dating of white micas from an Alpine high-pressure metamorphic belt on Naxos (Greece): resetting of the argon isotopic system. *Contributions to Mineralogy and Petrology*, **93**, 187–194.

WIJBRANS, J. R. & MCDOUGALL, I. 1988. Metamorphic evolution of the Attic-Cycladic metamorphic belt on Naxos (Cyclades, Greece). *Journal of Metamorphic Geology*, **6**, 571–594.

WIJBRANS, J. R., SCHLIESTEDT, M. & YORK, D. 1990. Single grain argon laser probedating of phengites from the blueschist to greenschist transition on Sifnos (Cyclades, Greece). *Contributions to Mineralogy and Petrology*, **104**, 582–593.

WILL, T., OKRUSCH, M., SCHMÄDICKE, E. & CHEN, G. 1998. Phase relations in the greenschist-blueschist-amphibolite-eclogite facies in the system Na_2O-CaO-FeO-MgO-Al_2O_3-SiO_2-H_2O (NCFMASH), with application to metamorphic rocks from Samos, Greece. *Contributions to Mineralogy and Petrology*, **132**, 85–102.

WILLETT, S. D., BEAUMONT, C. & FULLSACK, P. 1993. Mechanical model for the tectonics of doubly vergent compressional orogens. *Geology*, **21**, 371–374.

YARDLEY, B. W. D. 1989. *An introduction to metamorphic petrology*. Wiley, New York.

Received 13 October 2000; revised typescript accepted 13 June 2001.
Scientific editing by Mike Fowler.